Monthly Notices of the ROYAL ASTRONOMICAL SOCIETY

MNRAS **500,** 4678–4684 (2021) doi:10.1093/mnras/staa3527
Advance Access publication 2020 November 13

On the geometry and environment of repeating FRBs

Shuang Du [1,2]★ Weihua Wang,[1,2] Xuhao Wu[1,2] and Renxin Xu[1,2]★

[1]*State Key Laboratory of Nuclear Physics and Technology, School of Physics, Peking University, Beijing 100871, China*
[2]*Kavli Institute for Astronomy and Astrophysics, Peking University, Beijing 100871, China*

Accepted 2020 November 9. Received 2020 November 8; in original form 2020 May 18

ABSTRACT

We propose a geometrical explanation for periodically and non-periodically repeating fast radio bursts (FRBs) under neutron star (NS)–companion systems. We suggest a constant critical binary separation, r_c, within which the interaction between the NS and companion can trigger FRBs. For an elliptic orbit with the minimum and maximum binary separations, r_{min} and r_{max}, a periodically repeating FRB with an active period could be reproduced if $r_{min} < r_c < r_{max}$. However, if $r_{max} < r_c$, the modulation of orbital motion will not work due to persistent interaction, and this kind of repeating FRBs should be non-periodic. We test relevant NS–companion binary scenarios on the basis of FRB 180916.J0158+65 and FRB 121102 under this geometrical frame. It is found that the pulsar–asteroid belt impact model is more suitable to explain these two FRBs since this model is compatible with different companions (e.g. massive stars and black holes). At last, we point out that FRB 121102-like samples are potential objects that can reveal the evolution of star-forming region.

Key words: pulsars: general – galaxies: star formation – fast radio bursts.

1 INTRODUCTION

The origin of fast radio bursts (FRBs; Lorimer et al. 2007; Thornton et al. 2013) is still mysterious (see Katz 2018; Petroff, Hessels & Lorimer 2019 for reviews) but observations continue to refresh the understanding of FRBs. For example, the recent detection of a ∼16 d period from FRB 180916.J0158+65 indicates the progenitor of this FRB may be either a neutron star (NS)–companion binary or a precessing NS (Chawla et al. 2020; The CHIME/FRB Collaboration et al. 2020a) since the size of a non-relativistically moving source should be smaller than $\sim 10^7$ cm as evident from FRB durations.[1] The follow-up observation of the previous non-periodically repeating FRB 121102 (Spitler et al. 2016) shows that this FRB should also be a periodically repeating FRB (Cruces et al. 2020; Rajwade et al. 2020). These two observations bring up a question that are all repeating FRBs (even all FRBs) periodically repeating ones? Before this problem is understood, we still treat FRBs as three types: one-off bursts, non-periodically repeating bursts, and periodically repeating bursts.

Based on the different repeatability of FRBs, many progenitor models involving NSs have been proposed, e.g.

(1) for one-off bursts: binary NS mergers (Totani 2013), collapsing NSs (Falcke & Rezzolla 2014), and asteroids/comets colliding with NSs (Geng & Huang 2015);

(2) for non-periodically repeating bursts: magnetar hyperflares (Lyubarsky 2014), close NS–white dwarf binaries (Gu et al. 2016), and NSs 'combed' by plasma streams (Zhang 2017);

(3) for periodically repeating bursts: asteroid belts colliding with NSs (Dai et al. 2016) in tight O/B–star binaries (Lyutikov, Barkov & Giannios 2020), orbital-induced precessing NSs (Yang & Zou 2020), free/radiative precessing NSs (Zanazzi & Lai 2020), and precessing flaring magnetars (Levin, Beloborodov & Bransgrove 2020).

Besides, some of the models (e.g. Dai et al. 2016; Gu et al. 2016; Zhang 2017) used to explain the early observation of FRB 121102 (Spitler et al. 2016) have been revised to reproduce the periodicity detected in FRB 180916.J0158+65 (e.g. Dai & Zhong 2020; Gu, Yi & Liu 2020; Ioka & Zhang 2020).[2] These models usually focus on the observations that are related to FRB bursts themselves (e.g. duration, luminosity, and period) and do not consider the observations that may reveal the environment of FRBs [e.g. the changed/unchanged rotation measure (RM); Katz 2018; Michilli et al. 2018; Petroff et al. 2019].

Inspired by the consensus that long and short gamma-ray bursts are produced by similar compact star–accretion disc systems that originate from different progenitors (massive stars and NS binaries), in this paper, we propose a general geometrical frame of NS–companion systems to explain both periodically and non-periodically repeating FRBs without considering a detailed radiation mechanism. Then we will study the implications of this framework on relevant FRB models.

The remainder of this paper is organized as follows. The details of our model (the geometry, kinematics, and effect of orbital motion) are illustrated in Section 2. The case studies of FRB 180916.J0158+65

★ E-mail: dushuang@pku.edu.cn (SD); r.x.xu@pku.edu.cn (RX)

[1]In principle, black hole binaries (the present model of black hole binaries applies to one-off FRBs; see Zhang 2016) and accreting black holes with precessing jets (Katz 2020) could also provide the small-scale radiation regions and periods of periodically repeating FRBs. At present, no certain mechanism and observation show a strong coherent and millisecond-duration radio pulse can be emitted from these systems.

[2]Dai & Zhong (2020) have already constrained the structure of the NS–asteroid belt system according to the period of FRB 180916.J0158+65.

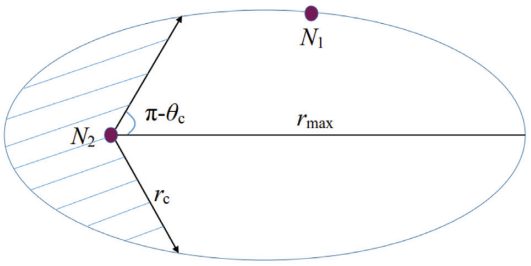

Figure 1. Schematic diagram of the geometry of our model. N_1 is the NS and N_2 is the companion. r_c is the constant critical binary separation (corresponding to the polar angle θ_c) under which the interaction between the NS and companion can trigger FRBs. r_{max} is the maximum binary separation. When the NS N_1 moves into the shaded region on the left, the binary begin to interact, so that FRBs are produced.

and FRB 121102 are shown in Section 3. We discuss the results of the two case studies in Section 4. Summary is presented in Section 5.

2 THE GEOMETRICAL MODEL

2.1 Orbital geometry

For an NS–companion binary with an orbital period T (see Fig. 1), we assume there is an approximately constant critical binary separation r_c (corresponding to the polar angle θ_c) under which the interaction between the NS N_1 and its companion N_2 can trigger bursts of a repeating FRB. When $r_c < r < r_{max}$ with r_{max} being the maximum separation between the binaries, there is no interaction between the orbiting objects and the FRB is in quiescence. For $r < r_c < r_{max}$, interaction between the companions will give rise to FRBs until r becomes greater than r_c. For $r_c > r_{max}$, interaction will be persistent and will result in FRBs that are emitted throughout the orbit, resulting in non-periodic repeating FRBs.[3]

So far, no periodicity has been detected between successive pulses of repeating FRBs. This indicates the radio emission of FRBs is not a 'lighthouse'. The radiation should not come from the NS polar cap but from a position in the NS magnetosphere that can always be seen by the observer. Correspondingly, the repeatability of a periodically repeating FRB during one orbital period should be mainly determined by the activity of the companion under this geometric frame. Note that the repeatability of non-periodically repeating FRBs does not depend on other geometric conditions as long as the condition $r_{max} < r_c$ is satisfied. We will only discuss the geometric details of periodically repeating FRBs in the next subsection.

2.2 Kinematics

According to Kepler's second law, an elliptic orbit can be described by

$$r = \frac{4\pi^2 m_\mu a^2 b^2}{\alpha T^2}\frac{1}{1+\varepsilon\cos\theta}, \tag{1}$$

$$a = \left(\frac{\alpha T^2}{4\pi^2 m_\mu}\right)^{1/3}, \tag{2}$$

[3]If the trajectory is a parabola, this non-periodically repeating FRB should be an 'one-off' repeating FRB.

and

$$b = a\sqrt{1-\varepsilon^2}, \tag{3}$$

where m_μ is the reduced mass of the binary (i.e. $m_1 m_2/(m_1+m_2)$ with m_1 being the mass of the NS and m_2 being the mass of the companion), a is the semimajor axis, b is the semiminor axis, α is defined as Gm_1m_2 with G the gravitation constant, θ is the polar angle, and ε is the orbital eccentricity.

In this geometrical framework, for a repeating FRB to have a period T with an active window of ΔT, there should be

$$\frac{\Delta T}{T}\pi ab = \int_0^{\theta_c} r^2\,\mathrm{d}\theta. \tag{4}$$

Integrating equation (4) gives

$$\frac{\Delta T}{T}\pi ab = \left(\frac{4\pi^2 m_\mu a^2 b^2}{\alpha T^2}\right)^2 \left[\frac{A+B}{AB\sqrt{AB}}\arctan\left(\sqrt{\frac{B}{A}}\tan\frac{\theta}{2}\right) - \frac{(A-B)\tan\frac{\theta}{2}}{AB\tan^2\frac{\theta}{2}+A^2}\right]\Bigg|_0^{\theta_c}, \tag{5}$$

with $A = 1+\varepsilon$ and $B = 1-\varepsilon$.

Note that T and ΔT are observable quantities, if m_1, m_2, and ε are known quantities, then one can solve θ_c, as well as the correspondingly critical binary separation r_c, numerically through equation (5).

2.3 The effect of the orbital motion

The orbital motion will change the binary separation, as well as the distance from the binary to the earth. Therefore, by definition, the RM and dispersion measure (DM) could be time-varying. For clarity, one can separate the contribution of orbital motion to the total RM and DM from observations, i.e.

$$\mathrm{RM} = \left(\frac{e^3}{2\pi m_e^2 c^4}\right)\left(\int_0^{l_c} n_e B_\parallel\,\mathrm{d}l + \int_{l_c}^{d} n_e{}' B_\parallel{}'\,\mathrm{d}l'\right) \tag{6}$$

and

$$\mathrm{DM} = \int_0^{l_c} n_e\,\mathrm{d}l + \int_{l_c}^{d} n_e{}'\,\mathrm{d}l', \tag{7}$$

where e and m_e are the charge and electron mass, $B_{\shortparallel}$ is the magnetic field along the line of sight, d is the shortest distance between the earth and the point in the orbit, and l_c is the orbital-motion-induced change in distance d. Since there is an inclination angle ι between the normal of the orbit and the line of sight, one has $2b\sin\iota \le l_c \le 2a\sin\iota$. From equations (6) and (7), the change in RM is

$$\Delta\mathrm{RM} = \left(\frac{e^3}{2\pi m_e^2 c^4}\right)\int_0^{l_c} n_e B_\parallel\,\mathrm{d}l. \tag{8}$$

By the definition that $\Delta\mathrm{DM} = \int_0^{l_c} n_e\,\mathrm{d}l$ and $\bar{B}_\parallel\Delta\mathrm{DM} = \int_0^{l_c} n_e B_\parallel\,\mathrm{d}l$, equation (8) can be rewritten as

$$\Delta\mathrm{RM} = \left(\frac{e^3\bar{B}_\parallel}{2\pi m_e^2 c^4}\right)\Delta\mathrm{DM}. \tag{9}$$

Equation (9) predicts that if l_c is large enough, ΔRM and ΔDM may change evidently during an orbital period as long as n_e and $B_{\shortparallel}$ are non-negligible.

Empirically, one can adopt $B_{\shortparallel} = B_{\shortparallel,0}(l/l_0)^{-p}$ and $n_e = n_{e,0}(l/l_0)^{-q}$ with l_0 being the size of the source that provides the magnetic environment. Given a point source, there should be $l_0 \ll l_c$. According

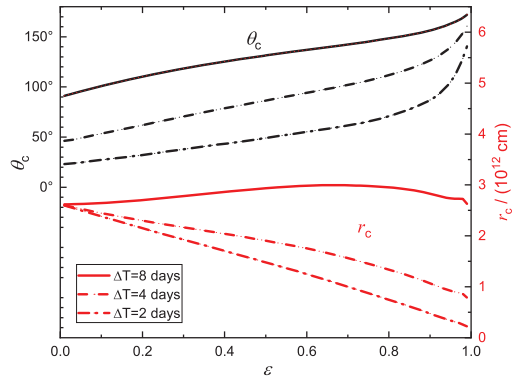

Figure 2. The values of θ_c and r_c versus ε under $T = 16$ d. The top three lines are θ_c versus ε. The three lines at the bottom are r_c versus ε. The solid lines, dashed lines, and dot–dashed lines are for $\Delta T/T = 1/2$, $\Delta T/T = 1/4$, and $\Delta T/T = 1/8$, respectively. Note that, from equations (1)–(3), there is a relation that $r_c \propto (m_1 + m_2)^{1/3} T^{2/3}$. Therefore, one can estimate r_c for a given binary through this relation and this figure.

to equation (6) and (7), one approximately has

$$\left(\frac{\bar{B}_{\parallel} n_{e,0} e^3}{2\pi m_e^2 c^4}\right) \int_{l_0}^{l_c} (l/l_0)^{-q}\, \mathrm{d}l \approx \left(\frac{B_{\parallel,0} n_{e,0} e^3}{2\pi m_e^2 c^4}\right) \int_{l_0}^{l_c} (l/l_0)^{-p-q}\, \mathrm{d}l. \quad (10)$$

Integrating equation (10) gives

$$B_{\parallel,0} \approx \bar{B}_{\parallel} \frac{p+q-1}{1-q} \left(\frac{l_c}{l_0}\right)^{-q+1} \quad (11)$$

under $0 < q < 1$, $-p - q + 1 < 0$, and

$$B_{\parallel,0} \approx \bar{B}_{\parallel} \frac{p+q-1}{q-1} \quad (12)$$

under $q > 1$, $-p - q + 1 < 0$.

Equations (9) and (10) indicate that the changes in RM and DM may provide the information of magnetic environment of periodically repeating FRBs. In the next, we will study two FRB samples on the basis of the above discussion.

3 TWO CASE STUDIES

3.1 FRB 180916.J0158+65

FRB 180916.J0158+65 shows a period of $T \approx 16$ d and an active period of $\Delta T \approx 4$ d (The CHIME/FRB Collaboration et al. 2020a). According to equations (1) and (5), the values of θ_c and r_c versus e are shown in Fig. 2 (see Appendix A for more details) by assuming the companion also is an NS and $m_1 = m_2 = 1.4\,M_\odot$. Since the companion may also be a massive star/black hole/white dwarf, we discuss these scenarios separately.

Under this geometrical frame, the interaction between the NS and companion (e.g. the accretion/wind interaction) should provide an approximately constant critical separation r_c. For the NS–massive star binary scenario, the accretion/wind interaction is susceptible to the activity of the massive star, so that the critical separation r_c may not be constant with time. The spin-down power of an NS is nearly a constant, as well as the critical separation induced by this wind interaction. Therefore, as the companion, an NS is worthy of consideration.

Under NS–NS scenario, the wind from the companion NS N_2 should be strong enough to 'comb' the NS N_1 (Zhang 2020), i.e.

$$\frac{L_{sd,2}}{4\pi r_2^2 c} = \frac{B_{p,1}^2}{8\pi} \left(\frac{R_*}{r_1}\right)^6, \quad (13)$$

where r_1 and r_2 are distances of the interaction front from NSs N_1 and N_2, respectively, $L_{sd,2}$ is the spin-down power of NS N_2, $B_{p,1}$ and R_* are the polar cap magnetic field and radius of NS N_1, and c is the speed of light. The typical isotropic value of repeating FRBs, $E_{FRB,iso}$, is a few 10^{41} erg s^{-1} (Luo et al. 2020). In principle, the rotational energy of the NS can satisfy this energy requirement but there is no clear mechanism to extract this energy through such an interaction between the two NSs. We turn to consider magnetic energy (which can be dissipated through magnetic reconnection). The magnetic-energy density of NS N_1 at r_1 should be high enough, i.e.

$$(c\Delta t)^3 \frac{B_{p,1}^2}{8\pi} \left(\frac{R_*}{r_1}\right)^6 \sim f_b E_{FRB,iso}, \quad (14)$$

where Δt is the duration of a FRB burst, and f_b is the beaming factor. Equation (14) gives

$$B_{p,1} \sim 3 \times 10^{12} \left(\frac{f_b E_{FRB,iso}}{10^{40}\,\mathrm{erg}}\right) \left(\frac{\Delta t}{1\,\mathrm{ms}}\right)^{-3} \left(\frac{r_1}{10^7\,\mathrm{cm}}\right) \mathrm{G}, \quad (15)$$

where $R_* = 10^6$ cm is adopted for the estimation.

According to equation (15), r_1 should be much smaller than r_c (e.g. $r_1 \sim c\Delta t$), otherwise $B_{p,1}$ will be too strong. Correspondingly, r_2 is given by

$$r_2 = r_c - r_1 \sim r_c - c\Delta t \sim r_c \sim 10^{12}\,\mathrm{cm}. \quad (16)$$

However, this brings up another problem that the magnetic field of NS N_2 would be unreasonable unless there is a very small f_b,[4] because, according to equation (13), there is

$$L_{sd,2} \sim 4\pi r_2^2 c \frac{f_b E_{FRB,iso}}{c^3 \Delta t^3} \sim 10^{53} \left(\frac{f_b E_{FRB,iso}}{10^{40}\,\mathrm{erg}}\right) \left(\frac{\Delta t}{1\,\mathrm{ms}}\right)^{-3} \mathrm{erg\,s^{-1}}. \quad (17)$$

Equation (17) shows the NS N_2 must be a millisecond magnetar with $B_{p,1} \sim 10^{16}$ G. This powerful wind only can last for <1 s since the largest rotational energy of an NS is $\sim 10^{52}$ erg.

For the NS–black hole binary scenario, both the accretion interaction and wind interaction require an accreting black hole. However, the changes in the accretion disc can result in changes in r_c. Besides, the luminosity of a super-Eddington accreting black hole is much smaller than that of a millisecond magnetar (see equation 17), so the wind from this accreting black hole is not strong enough to perturb the magnetosphere of NS N_1.

For the NS–white dwarf scenario, the wind from the white dwarf is much weaker. FRB bursts should be triggered by the accretion interaction. Since white dwarfs do not have mass ejections and bursts as the Sun, the accretion interaction between the NS and white dwarf could be different from that of the NS–massive star scenario. The separation r_c under this case may be approximately a constant. However, for the specific NS–white dwarf binary model (Gu et al. 2020), an extremely high eccentricity ($\varepsilon > 0.95$) is required to explain FRB 180916.J0158+65. This model demands the FRBs

[4]It is unrealistic since the size of the wind from the companion should be larger than the radius of NS N_1. Half of the magnetosphere of NS N_1 should be disturbed.

with $T > 16$ d to be special ones. Therefore, it can be tested after enough periodically repeating FRBs are detected.

In summary, the above discussion shows that the NS–massive star binary scenario cannot provide a constant r_c; the NS–NS binary scenario and NS–black hole binary scenario cannot provide strong winds; and the NS–white dwarf binary model (Gu et al. 2020) requires a special orbit with extremely high eccentricity. These models cannot explain all the observed characteristics of FRBs.

However, it is worth noting that the accretion/wind interaction is not the only way to provide a critical separation as long as the above stellar-mass objects have asteroid belts. Under the pulsar–asteroid belt impact model (Dai et al. 2016; Dai & Zhong 2020), the outer boundary of the asteroid belt is naturally corresponding to the critical separation r_c. Besides, there is another critical radius, r_c', i.e. the inner radius of the asteroid belt. If the trajectory of the NS can cross the inner boundary, the asteroid belt will divide the binary separation into three segments, i.e. $r < r_c'$, $r_c' < r < r_c$, and $r_c < r$. Therefore, there will be two periodic active phases that are separated by a quiescent phase during one orbital period. We suggest to fold periodically repeating FRBs at their period just like that of The CHIME/FRB Collaboration et al. (2020a). If such a FRB is found, the other FRB models should at least complement the corresponding details (e.g. for precessing NS models, the precession angle of the FRB beam is larger than the opening angle of the FRB beam). On the other hand, there is a tiny probability that the orbit of the NS N_1 happens to be in the asteroid belt (corresponding to $r_{max} < r_c$), so that the induced repeating FRB will show aperiodicity. Hence, the NS–asteroid belt model predicts that the number of aperiodically repeating FRBs will be much less than the periodically repeating ones.

So far, no observation shows that the RM and DM of FRB 180916.J0158+65 have obvious evolution. If the RM and DM of FRB 180916.J0158+65 are almost constants, according to equation (8), there are two explanations: (a) l_c is small enough; (b) n_e and $B_{\shortparallel}$ are negligible. Given $2b \sin\iota \leq l_c \leq 2a \sin\iota$, l_c can only be neglected when ι is very small (the orbit happens to be face-on). So, l_c is more likely a non-negligible quantity. The explanation (b) should be more reasonable, i.e. the companion is at least weak magnetized (e.g. a massive star/black hole). Alternatively, if future follow-up observation confirms this unchanged RM and DM, the single precessing NS scenario (corresponding to explanation (a); see e.g. Levin et al. 2020; Zanazzi & Lai 2020) is more suitable for explaining this observation.

3.2 FRB 121102

FRB 121102 is the first localized FRB (Tendulkar et al. 2017). The long-time follow-up observation shows that FRB 121102 also is a periodically repeating FRB with $T \sim 160$ d and $\Delta T \sim 76$ d (Cruces et al. 2020; Rajwade et al. 2020). Note that $r_c \propto (m_1 + m_2)^{1/3} T^{2/3}$ and r_c is not sensitive to ε (see Fig. 2) when $\Delta T/T \sim 1/2$. For an NS binary scenario, there is $r_c \sim 7 \times 10^{13}$ cm. Comparing with the case of FRB 180916.J0158+65, this time the accretion/wind interaction must be stronger since l_c gets longer. Therefore, under the wind interaction, the NS–NS binary and NS–black hole binary scenarios are more powerless to explain FRB 121102 according to the discussion in Section 3.1. Under the accretion interaction, the interaction between the NS and white dwarf should work on a longer distance. Besides, the longer period of FRB 121102 indicates a much larger eccentricity and a much smaller white dwarf for the certain NS–white dwarf binary model (this is unreasonable; see fig. 2 of Gu et al. 2020). Comparing with the above scenarios and models, the pulsar–asteroid belt impact model seems to be not quite that extreme (it needs a huge asteroid belt; see Smallwood, Martin & Zhang 2019).

Observations have shown that the RM of FRB 121102 changed from 1.46×10^5 rad m^{-2} to 1.33×10^5 rad m^{-2} within 7 months (Michilli et al. 2018). The recent work shows that the RM of FRB 121102 has a consistent decreasing trend in RM with the DM being steadily increasing (Hilmarsson et al. 2020). Thus, despite the orbital motion could induce the change in RM, this effect should not be the primary cause since the orbital period is much shorter than the duration of the decrease in RM. Nevertheless, we can use the published data (Michilli et al. 2018) to estimate the upper limit, $B_{\shortparallel,0,max}$, of $B_{\shortparallel,0}$. We will roughly adopt $l_c \sim r_c$ (see the last paragraph of Section 3.1) for the following estimation.

Away from a point source, the radial component of the magnetic field decays as l^{-2}, and the toroidal component decays as l^{-1}, i.e. $1 < p < 2$ (see e.g. Spruit, Daigne & Drenkhahn 2001). On the other hand, q should be $\sim$0 for intergalactic medium and $\sim$2 for stellar wind. In any case, the middle term of the right-hand side of equation (11) is larger than 1. Therefore, $\bar{B}_{\shortparallel}$ should be small enough to keep the value of $B_{\shortparallel,0}$ reasonable (see equation 11). From equation (9), there is (see also Katz 2018)

$$\bar{B}_{\shortparallel} = \left(\frac{2\pi m_e^2 c^4}{e^3}\right)\frac{\Delta \mathrm{RM}}{\Delta \mathrm{DM}} = 67.6\left(\frac{\Delta \mathrm{RM}}{10^4\,\mathrm{rad\,m^{-2}}}\right)\left(\frac{3\,\mathrm{pc\,cm^{-3}}}{\Delta \mathrm{DM}}\right)\mathrm{mG}. \quad (18)$$

Since ΔRM induced by the orbital motion should be smaller than $1.46 \times 10^5 - 1.33 \times 10^5 = 1.3 \times 10^4$ rad m^{-2}, we can estimate $B_{\shortparallel,0,max}$ under different companions through equations (11), (12), and (18).

Under the intergalactic medium situation, the results are as follows.

(i) For the NS–NS binary scenario, there is $l_0 \sim 10^6$ cm. So one has

$$B_{\shortparallel,0,\max} \sim 5.2 \times 10^5 \left(\frac{\Delta \mathrm{DM}}{3\,\mathrm{pc\,cm^{-3}}}\right)^{-1}\left(\frac{l_c}{10^{13}\,\mathrm{cm}}\right)\mathrm{G}. \quad (19)$$

However, observations[5] show that the magnetic field of the NS in an NS–NS binary is stronger than 10^9 G. Therefore, the magnetic field of an NS is too large for equations (19).[6]

(ii) For the NS–massive star binary scenario, we adopt $l_0 \sim 10^{11}$ cm. Then one has

$$B_{\shortparallel,0,\max} \sim 5.2\left(\frac{\Delta \mathrm{DM}}{3\,\mathrm{pc\,cm^{-3}}}\right)^{-1}\left(\frac{l_c}{10^{13}\,\mathrm{cm}}\right)\mathrm{G}. \quad (20)$$

This value is compatible with the magnetic field of a massive star (Bychkov, Bychkova & Madej 2009).

(iii) For the NS–white dwarf binary scenario, $l_0 \sim 10^8$ cm is adopted for estimation. There is

$$B_{\shortparallel,0,\max} \sim 5.2 \times 10^3 \left(\frac{\Delta \mathrm{DM}}{3\,\mathrm{pc\,cm^{-3}}}\right)^{-1}\left(\frac{l_c}{10^{13}\,\mathrm{cm}}\right)\mathrm{G}. \quad (21)$$

This value also is compatible with observations (Tout et al. 2008).

(iv) If the companion is a black hole, the magnetic field should be provided by the accretion disc. We adopt the outer boundary of the

[5]Data come from the Australia Telescope National Facility (ATNF) Pulsar Database (Manchester et al. 2005; https://www.atnf.csiro.au/research/pulsar/psrcat/).

[6]Even if the value of ΔDM is taken as $\sim$0.1 (The CHIME/FRB Collaboration et al. 2020a), the value of $B_{\shortparallel,0}$ is still much smaller than 10^9 G.

disc $\sim 50 r_{\rm g}$ with $r_{\rm g}$ being the Schwarzschild radius of the black hole. The result is

$$B_{\parallel,0,\max} \sim 17 \left(\frac{\Delta {\rm DM}}{3\,{\rm pc\,cm^{-3}}}\right)^{-1} \left(\frac{l_{\rm c}}{10^{14}\,{\rm cm}}\right) \left(\frac{M_{\rm BH}}{10^3\,{\rm M_\odot}}\right)^{-1} {\rm G}, \quad (22)$$

where $M_{\rm BH}$ is the mass of the black hole. This value is consistent with previous work (e.g. Ferreira & Pelletier 1995).

Under the stellar wind situation, the value of $B_{\parallel,0}$ is independent of the companion (see equation 12). Since the magnetic field of an NS or a white dwarf is too large for equation (18), the companion should be a massive star or a black hole.

4 COMPARISON OF THE TWO CASE STUDIES

Based on the study of FRB 180916.J0158+65 presented in the previous section, if the FRB is induced by the accretion/wind interaction, the companion should not be a massive star or an NS; the companion star could be a white dwarf only if FRB 180916.J0158+65 is a special one. The unchanged RM of FRB 180916.J0158+65 indicates the companion should be weakly magnetized. Under the pulsar–asteroid belt impact model, the companion could be a massive star/black hole as long as the companion has an asteroid belt.

The case study of FRB 121102 shows that the feasibilities of scenarios involving accretion/wind interaction (e.g. NS–NS/white dwarf binary scenario) need some unreasonable conditions due to the larger period T and critical separation $r_{\rm c}$. The pulsar–asteroid belt impact model could reproduce the observed T, ΔT, and satisfy the change in RM more reasonably (the asteroid belt should be large enough) due to the compatibility with different companions, e.g. massive stars and black holes.

In Section 3.2, we mention that orbital motion is not the primary cause to induce the change in the RM of FRB 121102. Since the source of FRB 121102 is colocated with a star-forming region (Bassa et al. 2017), the gases in the star-forming region may mainly induce the change in the RM of FRB 121102.[7] Therefore, the following discussion can also be applied to the precessing NS scenario since the change in the RM is induced by the evolution of the star-forming region and has nothing to do with the FRB source. Let us check this idea at first.

The RM contributed by the star-forming region is given by

$${\rm RM_g} = \left(\frac{e^3}{2\pi m_{\rm e}^2 c^4}\right) \int_0^{l_{\rm g}} n_{\rm e,g} B_{\parallel,{\rm g}}\,{\rm d}l, \quad (23)$$

where $l_{\rm g}$ is the size scale of the gases along the line of sight, and $n_{\rm e,\,g}$ and $B_{\parallel,{\rm g}}$ are number density of electrons and magnetic field strength along the line of sight in the gases, respectively. To reproduce the observed RM, from equation (23), the magnetic field strength over the size scale $l_{\rm g}$ should be

$$B_{\parallel,{\rm g}} \sim 12.3 \left(\frac{\rm RM}{10^5\,{\rm rad\,m^{-2}}}\right) \left(\frac{l_{\rm g}}{100\,{\rm pc}}\right)^{-1} \left(\frac{n_{\rm e,g}}{100\,{\rm cm^{-3}}}\right)^{-1} \mu{\rm G}. \quad (24)$$

If this magnetic field is provided by the dynamo process in the gases,

$$\frac{B_{\parallel,{\rm g}}^2}{4\pi} < \frac{1}{2} n_{\rm p} m_{\rm p} v_{\rm p}^2, \quad (25)$$

where $n_{\rm p}$ and $v_{\rm p}$ are the number density of protons and velocity of the gases, respectively, and $m_{\rm p}$ is the proton mass. According to equations (24) and (25), there is

$$n_{\rm p} > 12 \left(\frac{B_{\parallel,{\rm g}}}{12.3\,\mu{\rm G}}\right)^2 \left(\frac{v_{\rm p}}{10^6\,{\rm cm\,s^{-1}}}\right)^{-2} {\rm cm^{-3}}. \quad (26)$$

Through equations (24) and (26), one can find that $n_{\rm p}$ is compatible with $n_{\rm e}$. Therefore, this idea is self-consistent.

If the total RM is mainly contributed by the star-forming region, according to equation (23), the change in RM should be induced by the changes in $l_{\rm g}$, $n_{\rm e,\,g}$, and $B_{\parallel,{\rm g}}$. This demands

$$\Delta {\rm DM} = \int_0^{l_{\rm g}(0)} n_{\rm e,g}(l,t)\,{\rm d}l - \int_0^{l_{\rm g}(t)} n_{\rm e,g}(l,t)\,{\rm d}l \ll {\rm DM}, \quad (27)$$

$$\frac{{\rm dRM}}{{\rm d}t} \approx \left(\frac{e^3}{2\pi m_{\rm e}^2 c^4}\right) \frac{\rm d}{{\rm d}t} \left[\int_0^{l_{\rm g}(t)} n_{\rm e,g}(l,t) B_{\parallel,{\rm g}}(l,t)\,{\rm d}l\right], \quad (28)$$

where t is the time since the first measurement of RM. Note that

$$\frac{\Delta {\rm DM}}{\rm DM} \ll \frac{\Delta {\rm RM}}{\rm RM}, \quad (29)$$

${\rm DM_g} = \int_0^{l_{\rm g}(t)} n_{\rm e,g}(l,t)\,{\rm d}l$ can be approximately treated as a constant (see equation 27). Therefore, equation (28) is reduced to

$$\begin{aligned}\frac{{\rm dRM}}{{\rm d}t} &\approx \left(\frac{e^3}{2\pi m_{\rm e}^2 c^4}\right) \frac{\rm d}{{\rm d}t} \left[{\rm DM_g} \bar{B}_{\parallel,{\rm g}}(t)\right] \\ &= \left(\frac{e^3}{2\pi m_{\rm e}^2 c^4}\right) {\rm DM_g} \frac{\rm d}{{\rm d}t} \left[\bar{B}_{\parallel,{\rm g}}(t)\right], \end{aligned} \quad (30)$$

where $\bar{B}_{\parallel,{\rm g}}$ has the same definition as that of $\bar{B}_{\parallel}$. So, once the time evolution of RM is determined by future observations, one can infer the time evolution of $\bar{B}_{\parallel,{\rm g}}$ through equation (30). FRB 121102-like samples may be potential objects that can probe the evolution of star-forming regions in distant galaxies (e.g. turbulence and convection).

5 SUMMARY

In this paper, we show a general geometrical frame to explain the periodically and non-periodically repeating FRBs. We study FRB 180916.J0158+65 and FRB 121102 under this geometrical frame and find that the pulsar–asteroid belt impact model is preferred (although a huge asteroid belt is needed; Smallwood et al. 2019; Dai & Zhong 2020). Besides, we point out that FRB 121102-like samples may be potential objects that can reveal the evolution of star-forming region.

Although we concentrate on the geometrical frame of NS–companion systems in this paper, it is worth reminding that the precessing NS scenario is more suitable for explaining a repeating FRB with an unchanged RM. We also discuss a possible explanation to the changed RM of FRB 121102 under the precessing NS scenario in Section 4. This is only one aspect of the problem. The invoking of a precessing NS is to produce a gyroscope-like radio beam so that the beam toward/outward Earth's field of view can also reproduce the observed periodicity (e.g. Levin et al. 2020; Zanazzi & Lai 2020). However, there is no conclusive evidence that shows that precession exists in the known isolated pulsars and magnetars on such short timescales till now.[8] Besides, the duty cycle $\Delta T/T$ depends on the size of the radio-emission region on the NS (see e.g. the pink semicircle in

[7] It is worth reminding that the source of FRB 180916.J0158+65 also is colocated with a star-forming region (Marcote et al. 2020). We should expect the correlation of locations between the star-forming region and the source of FRB 180916.J0158+65 to be different from that of FRB 121102. Another explanation to the higher RM of FRB 121102 can be found in Margalit et al. (2018) [the following discussion (e.g. equation x5) is still applicable].

[8] The spin–precession period induced by spin–orbit coupling is too long for periodically repeating FRBs (even for the most compact relativistic system: PSR J0737−3039; Burgay et al. 2003; Lyne et al. 2004).

fig. 3 of Zanazzi & Lai 2020). If the result of Rajwade et al. (2020) is confirmed, this scenario will face a problem that the emission region becomes unrealistic for a 160-d periodicity since $\Delta T/T$ is the ratio of the radio-emission region size to the circumference at the same latitude. Maybe, the free/radiative precessing NS model (Zanazzi & Lai 2020) needs a wider radio beam; and the precessing flaring magnetar model needs a wider 'pancake'-like plasmoid to produce a FRB beam with a larger solid angle (see the lower panel of fig. 1 in Levin et al. 2020).

Nevertheless, both the geometric frame and the model invoke a gyroscope-like radio beam have to explain the lack of FRBs in the Milky Way (see Appendix B for more discussions). There are three speculations for the no detection: (i) such a system should be a special one that belongs to 'rare species' so that the absolute quantity of these systems is much less than the number of NSs in the Milky Way; (ii) the radio emissions of these rare-species systems tend to be outward rather than along the Galactic disc so that the Galactic FRBs are difficult to be seen; (iii) the conditions for coherent radiation are hard to be satisfied (suitable magnetic field, position and charge density, etc.) since not every X-ray burst is corresponding to a radio burst.

In this paper, we do not discuss the detailed radiation mechanism of radio emission (e.g. Wang et al. 2019) since it depends on the unknown structure of NS magnetospheres and complicated magnetohydrodynamic processes. Although the details of radio radiation are unknown, this NS–companion frame can still be tested by detecting the gravitational-wave radiation induced by orbital inspiral (e.g. *Laser Interferometer Space Antenna* (*LISA*), Amaro-Seoane et al. 2017; *TianQin*, Luo et al. 2016; and *Taiji*, Ruan et al. 2020).

ACKNOWLEDGEMENTS

We acknowledge the use of the ATNF Pulsar Catalogue. We would like to thank the anonymous referee for very useful comments that have allowed us to improve our paper (e.g. the suggestion to estimate the effect of the change in r_c on $\Delta T/T$ and corrections of English expression). We would like to thank Mr Weiyang Wang for telling us that there is a 4-d active period of FRB 180916.J0158+65. This motivates us to construct such a geometric frame. We would like to thank Professor Yuefang Wu and Mr Heng Xu for useful discussion. This work was supported by the National Key Research and Development Program of China (Grant No. 2017YFA0402602), the National Natural Science Foundation of China (Grant Nos 11673002 and U1531243), and the Strategic Priority Research Program of Chinese Academy of Sciences (Grant No. XDB23010200).

DATA AVAILABILITY

The data that support the plots within this paper are available from the corresponding author upon reasonable request.

REFERENCES

Amaro-Seoane P. et al., 2017, preprint (arXiv:1702.00786)
Bassa C. G. et al., 2017, ApJ, 843, L8
Bochenek C. D., Ravi V., Belov K. V., Hallinan G., Kocz J., Kulkarni S. R., McKenna D. L., 2020, Nature, 587, 59
Burgay M. et al., 2003, Nature, 426, 531
Bychkov V. D., Bychkova L. V., Madej J., 2009, MNRAS, 394, 1338
Chawla P. et al., 2020, ApJ, 896, L41
Cruces M. et al., 2020, MNRAS, 500, 448
Dai Z. G., Zhong S. Q., 2020, ApJ, 895, L1
Dai Z. G., Wang J. S., Wu X. F., Huang Y. F., 2016, ApJ, 829, 27
Falcke H., Rezzolla L., 2014, A&A, 562, A137
Ferreira J., Pelletier G., 1995, A&A, 295, 807
Geng J. J., Huang Y. F., 2015, ApJ, 809, 24
Gu W. M., Dong Y.-Z., Liu T., Ma R., Wang J., 2016, ApJ, 823, L28
Gu W. M., Yi T., Liu T., 2020, MNRAS, 497, 1543
Hilmarsson G. H. et al., 2020, preprint (arXiv:2009.12135)
Ioka K., Zhang B., 2020, ApJ, 893, L26
Katz J. I., 2018, Progress Part. Nucl. Phys., 103, 1
Katz J. I., 2020, MNRAS, 494, L64
Levin Y., Beloborodov A. M., Bransgrove A., 2020, ApJ, 895, L30
Li C. K. et al., 2020, Nature, preprint (arXiv:2005.11071)
Lorimer D. R., Bailes M., McLaughlin M. A., Narkevic D. J., Crawford F., 2007, Science, 318, 777
Luo J. et al., 2016, Classical Quantum Gravity, 33, 035010
Luo R., Men Y., Lee K., Wang W., Lorimer D. R., Zhang B., 2020, MNRAS, 494, 665
Lyne A. G. et al., 2004, Science, 303, 1153
Lyubarsky Y., 2014, MNRAS, 442, L9
Lyutikov M., Barkov M., Giannios D., 2020, ApJ, 893, L39
Manchester R. N., Hobbs G. B., Teoh A., Hobbs M., 2005, AJ, 129, 1993
Marcote B. et al., 2020, Nature, 577, 190
Margalit B., Metzger B. D., 2018, ApJ, 868, 4
Mereghetti S. et al., 2020, ApJ, 898, L29
Michilli D. et al., 2018, Nature, 553, 182
Petroff E., Hessels J. W. T., Lorimer D. R., 2019, A&AR, 27, 4
Rajwade K. M. et al., 2020, MNRAS, 495, 3551
Ridnaia A. et al., 2020, preprint (arXiv:2005.11178)
Ruan W.-H., Guo Z.-K., Cai R.-G., Zhang Y.-Z., 2020, Int. J. Mod. Phys. A, 35, 2050075
Smallwood J. L., Martin R. G., Zhang B., 2019, MNRAS, 485, 1367
Spitler L. G. et al., 2016, Nature, 531, 202
Spruit H. C., Daigne F., Drenkhahn G., 2001, A&A, 369, 694
Tavani M. et al., 2020, Nature Astronomy, preprint (arXiv:2005.12164)
Tendulkar S. P. et al., 2017, ApJ, 834, L7
The CHIME/FRB Collaboration et al., 2020a, Nature, 582, 351
The CHIME/FRB Collaboration et al., 2020b, Nature, 587, 54
Thornton D. et al., 2013, Science, 341, 53
Totani T., 2013, PASJ, 65, L12
Tout C. A., Wickramasinghe D. T., Liebert J., Ferrario L., Pringle J. E., 2008, MNRAS, 387, 897
Wang W. Y., Zhang B., Chen X. L., Xu R. X., 2019, ApJ, 876, 15
Yang H., Zou Y.-C., 2020, ApJ, 893, L31
Zanazzi J. J., Lai D., 2020, ApJ, 892, L15
Zhang B., 2016, ApJ, 827, L31
Zhang B., 2017, ApJ, 836, L32
Zhang B., 2020, ApJ, 890, L24

APPENDIX A

From equations (1)–(3), there is

$$\frac{\partial r_c}{\partial \varepsilon} = \left(\frac{\alpha T^2}{4\pi^2 m_\mu}\right)^{1/3} \frac{\varepsilon^2 \cos\theta_c + 2\varepsilon + 1}{(1+\varepsilon\cos\theta_c)^2}. \quad \text{(A1)}$$

If changes in r_c on the size scale of an NS magnetosphere do not affect $\Delta T/T$, there should be a 'step length' of the eccentricity, $\Delta\varepsilon$, which satisfies

$$\frac{\partial r_c}{\partial \varepsilon}\Delta\varepsilon \sim \frac{2\pi c}{P_1}, \quad \text{(A2)}$$

where P_1 is the rotational period of the NS N_1. Combining equations (A1) and (A2), when the change in orbital eccentricity is within

$$\Delta\varepsilon \sim \frac{2\pi c}{P_1}\left(\frac{\alpha T^2}{4\pi^2 m_\mu}\right)^{-1/3} \frac{(1+\varepsilon\cos\theta_c)^2}{\varepsilon^2\cos\theta_c + 2\varepsilon + 1}, \quad \text{(A3)}$$

$\Delta T/T$ would be approximately a constant. Considering $r_c \sim 10^{11}$–10^{12} cm and $P_1 = 10^{-2}$–10^{-1} s, there is $\Delta\varepsilon \sim 10^2$–$10^4$ according to equation (A3). This is not a reasonable result since $\Delta\varepsilon$ must be smaller than 1. Under the geometrical frame, the unreasonable value of $\Delta\varepsilon$ indicates a small change in r_c can and must affect $\Delta T/T$.

APPENDIX B

We do not believe FRB 200428 (Bochenek et al. 2020; The CHIME/FRB Collaboration et al. 2020b) has the same origin as the cosmological FRBs. Before discussing this question further, we should specify that what an FRB is. If an FRB is just defined as a millisecond-duration bright radio pulse, it is fine to call the two radio pulses (Bochenek et al. 2020; The CHIME/FRB Collaboration et al. 2020b) as FRBs. However, once considering the physical origin, one should treat the differences between FRB 200428 (weaker luminosity and X-ray burst association) and cosmological FRBs more carefully, although the absence of FRB 200428-like cosmological FRBs can be naturally explained as a selection effect. Remember that soft gamma-ray repeaters (SGRs) are mistakenly believed to be gamma-ray bursts in history. If all FRBs are produced by the events that generate SGR bursts (Li et al. 2020; Mereghetti et al. 2020; Ridnaia et al. 2020; Tavani et al. 2020), it is difficult to reconcile the association between accidental SGR bursts and periodically repeating FRBs (unless the period origins from a certain 'external factor', e.g. asteroid belts). As the reviewer comments 'the fact that luminosity of the SGR burst is at least 30 times smaller than the faintest pulse of an FRB is a strong enough argument to suggest that not all repeaters may come from SGR-like origin'.

This paper has been typeset from a TEX/LATEX file prepared by the author.